

*John
Stet*

NASA
Technical
Paper
2059

November 1982

*Ruthie
S. Stet*

W.H.

Effect of Sliding Speed and Contact Stress on Tribological Properties of Ultra-High-Molecular- Weight Polyethylene

Robert L. Fusaro

DEPARTMENT OF DEFENSE
ELASTICS TECHNICAL EVALUATION CENTER
AMARILLO, TEXAS 79101

19951228 057

NASA

DISTRIBUTION STATEMENT A
Approved for public release;
Distribution Unlimited

ELASTEC
TECHNICAL
EVALUATION
CENTER

Date: 7/15/95 Time: 5:56:49PM

Page: 1 Document Name: untitled

1 OF 1

DTIC DOES NOT HAVE THIS ITEM

-- 1 - AD NUMBER: D436244
-- 5 - CORPORATE AUTHOR: NATIONAL AERONAUTICS AND SPACE ADMINISTRATION
-- CLEVELAND OH LEWIS RESEARCH CENTER
-- 6 - UNCLASSIFIED TITLE: EFFECTS OF SLIDING SPEED AND CONTACT STRESS
-- ON TRIBOLOGICAL PROPERTIES OF ULTRA-HIGH-MOLECULAR-WEIGHT
-- POLYETHYLENE.
-- 10 - PERSONAL AUTHORS: FUSARO, R. L.
-- 11 - REPORT DATE: NOV , 1982
-- 12 - PAGINATION: 21P
-- 14 - REPORT NUMBER: E-1060, NASA-TP-2059
-- 20 - REPORT CLASSIFICATION: UNCLASSIFIED
-- 22 - LIMITATIONS (ALPHA): APPROVED FOR PUBLIC RELEASE; DISTRIBUTION
-- UNLIMITED. AVAILABILITY: NATIONAL TECHNICAL INFORMATION SERVICE,
-- SPRINGFIELD VA 22161, NASA-TP-2059.
-- 33 - LIMITATION CODES: 1 24

**NASA
Technical
Paper
2059**

1982

Effect of Sliding Speed and Contact Stress on Tribological Properties of Ultra-High-Molecular- Weight Polyethylene

Robert L. Fusaro
*Lewis Research Center
Cleveland, Ohio*

LOW QUALITY INSPECTED BY



National Aeronautics
and Space Administration

Scientific and Technical
Information Branch

DISTRIBUTION STATEMENT A

Approved for public release;
Distribution Unlimited

Summary

The tribological properties of hemispherically tipped AISI 440C high-temperature (HT) stainless-steel riders (0.476-cm radius) sliding against ultra-high-molecular-weight polyethylene (UHMWPE) disks were studied. The riders were loaded against the UHMWPE disk by using a 9.8-N weight and were slid at speeds of 1, 10, 100, and 800 rpm (0.003 to 1.7 m/s) in a moist air atmosphere (10 000 ppm H₂O) at 25° C. Optical microscopy and surface profilometry were used to study the wear surface morphology and transfer film formation and growth. Observations were made at preset intervals throughout the experiments by stopping the tests and removing the specimens from the apparatus.

Friction coefficient increased with increasing sliding speed and with increasing sliding distance. Increasing friction coefficients were associated with decreasing contact stresses and with the buildup of thick "ridge like" transfer. Low friction coefficients occurred when thin, flowing transfer films were formed.

Although UHMWPE wear rate did not depend on sliding speed, different wear mechanisms occurred as speed changed. For the highest sliding speed (800 rpm) and for short sliding distances for the other speeds (1, 10, and 100 rpm), adhesive wear predominated. But for longer sliding distances at the lower sliding speeds, a fatigue-like wear process took place due to the buildup of "ridge like" rider transfer.

High contact stresses due to the hemispherical shape of the metallic rider induced plastic deformation of the UHMWPE disk until stresses fell to about 13 MPa. Below this stress level UHMWPE wear rate was not markedly affected by contact stress.

Another wear phenomenon occurred in one experiment. A hard-particle inclusion in the UHMWPE disk abrasively wore a groove in the metallic rider. The origin of the particle was unknown. In the absence of inclusions, no measurable wear took place on the metallic riders.

Introduction

Polymers and polymer-based composites are increasingly being used for tribological applications. For example, in the aerospace industry they are used in control bearings and in foil bearings (refs. 1 to 5). One particular polymer that has exceptional friction and wear properties is ultra-high-molecular-weight polyethylene (UHMWPE). UHMWPE is currently being employed with great success for the replacement of degenerative human joints, such as the hip, knee, and shoulder joints (refs. 6 to 8).

For ambient-temperature applications, such as the above, UHMWPE performs exceptionally well; however, because it does not possess good stability at temperatures greater than 93° C, it is not suitable for high-temperature applications. It is important though for the development of new polymers and polymer-based composites that will function at higher temperatures, speeds, and loads to better understand how polymers such as UHMWPE lubricate and wear.

This study was conducted to investigate the effect of different sliding speeds on the friction coefficient and wear rates and to determine the wear mechanisms of an AISI 440C high-temperature (HT) stainless-steel hemispherically tipped rider sliding against an UHMWPE disk. Transfer films and UHMWPE wear track surface morphology were studied in an effort to deduce lubricating and wear mechanisms. The effect of varying contact stresses on wear rate and friction coefficient was also investigated. The results were compared with the results of other researchers (refs. 8 and 9) who used different test configurations.

Materials

Rider specimens were made of AISI 440C HT stainless steel with a hardness of Rockwell C-58 and a surface finish of $0.09 \pm 0.02 \mu\text{m}$ cla (centerline average). The disks were made of ultra-high-molecular-weight polyethylene (UHMWPE). They were machined from a block of surgical-grade polymer (RCH 1000) manufactured and supplied by Hoechst A.G. The UHMWPE had a density of 0.937 kg/m³, a soluble weight-average molecular weight of 2 588 000, and a diamond pyramid hardness of $4.9 \pm 0.7 \text{ kg/mm}^2$ (ref. 9).

Apparatus

Two different pin-on-disk sliding friction and wear apparatuses were used to study the tribological properties of 0.476-cm-radius, hemispherically tipped AISI 440C HT stainless-steel riders sliding against 6.3-cm-diameter UHMWPE disks. They are shown in figures 1 and 2. The device in figure 1 was used only for the 800-rpm tests, and the device in figure 2 was used for the 1-, 10-, 100-, and 800-rpm tests. The riders were loaded with a 9.8-N deadweight against the flat UHMWPE disk at diameters of 4.0 to 6.0 cm; thus constant speeds of 0.003 to 1.7 m/s were maintained. The friction specimens were enclosed in chambers so that atmosphere could be controlled. To obtain an atmosphere of 10 000 ppm H₂O (50 percent relative humidity at 25° C), dry air was mixed with air bubbled through water.

Procedure

Surface Cleaning

The metal riders were washed with pure ethyl alcohol and then scrubbed with a water paste of levigated alumina. They were rinsed in distilled water and dried with compressed air.

The UHMWPE disks were scrubbed with a nonabrasive detergent, rinsed with distilled water, and dried with compressed air.

Friction and Wear Tests

The procedure for conducting the friction and wear tests was as follows: The rider and disk were inserted into the friction apparatus, and the test chamber was sealed. The test atmosphere, moist air (10 000 ppm H₂O), was purged through the chamber for 15 min before each test.

The flow rate was 1500 cm³/min, and the volume of the chamber was 2000 cm³. After the 15-min purge the disk was set into rotation at 1000 rpm and a 9.8-N load was gradually applied. The test temperature was 24° ± 3° C (ambient).

Each test was stopped either after 20 cycles (for sliding speeds of 100 rpm or less) or after 1000 cycles (for sliding speeds of 800 rpm). After the rider and disk were removed from the friction apparatus, the contact areas were examined by optical microscopy and photographed. Surface profiles of the disk wear tracks were also taken. The rider and disk were then placed back into the apparatus and the test procedure was repeated. The rider was not removed from the holder, and locating pins in the apparatus ensured that it was returned to its original position. Each test was stopped and this procedure repeated at various sliding intervals up to 10 000 kilocycles.

The experimental method used to determine the effect of speed was to first "run in" the specimens at 1 rpm for 20 min. Then a series of 5-min tests were performed at each of the following speeds: 0.25, 1, 10, 50, 100, 400, 800 rpm. The speed was first increased from 1 rpm to 800 rpm, then decreased to 0.25 rpm, and finally increased again to 800 rpm. Thus, for most of the speeds, three tests were made.

Analysis of Sliding Surfaces

Optical microscopy was used to study the wear surfaces, the transfer films, and the wear particles in this investigation. The surfaces were viewed at magnifications to 2000. At these high magnifications, the depth of focus was very small (1 μm); this feature was used in measuring the heights of various features on the sliding surfaces, such as transfer film thickness and wear track depth.

The microscope was also equipped with two polarizing filters (one that could be rotated); thus the sliding

surfaces could be examined between crossed polarizing filters. Birefringent particles observed by this method indicated that the particles had an anisotropic crystalline structure.

Results

Friction

Average friction coefficients are plotted in figure 3 as a function of sliding distance in cycles (1 cycle equals 0.13 to 0.19 m) for sliding speeds of 1, 10, 100, and 800 rpm. Average incremental values of the friction coefficients for each experiment are also given in table I. In general, the initial friction coefficient for any individual experiment was lower than its average value for the duration of the experiment. For sliding speeds of 10, 100, and 800 rpm, it took about 1000 cycles of sliding before the friction coefficient stabilized at 0.13 ± 0.03. The friction coefficient for the experiment conducted at 1 rpm remained constant at 0.05 ± 0.02 for the duration of the experiment (4300 cycles).

To investigate further the effect of sliding speed on the friction coefficient, an experiment was devised whereby the friction coefficient was measured at sliding speeds of 0.25 to 800 rpm all on the same wear track (see the section Procedure). Figure 4 gives those results, which indicate that both sliding duration and decreasing and increasing speed affected the friction coefficient. In general, however, the friction coefficient increased as speed was increased, although at speeds below 10 rpm the effect was minimal.

UHMWPE Wear

UHMWPE wear was studied by taking surface profiles of the disk wear track after each sliding interval. Figure 5 gives representative surface profiles for the 10-, 100-, and 800-rpm sliding speed tests after various sliding durations. Because the vertical magnification of the surface is about 40 times the horizontal magnification, the view of the surface is distorted.

The surface profiles show that the wear process was one of gradual wear through the UHMWPE disk. The profiles also show that some plastic deformation occurred at the sides of the wear track. Another interesting phenomenon is that the wear track surfaces on the UHMWPE disk for the 10- and 100-rpm tests (also for the 1-rpm test, which is not shown) were very rough; but for the tests at 800 rpm the surface was much smoother. Possible reasons for this are discussed in the section Surface Wear Morphology.

To quantify the wear process, wear was calculated by measuring the cross-sectional area of the wear tracks (from the surface profiles) after each sliding interval. At

least four different traces at different positions were taken at each interval. Wear volume was then calculated by multiplying the cross-sectional area by the circumference of the tracks. Figure 6 plots average wear volume as a function of sliding distance on a log-log scale.

Wear rate was determined for each sliding interval. These incremental wear rates are listed in table II and plotted in figure 7 as a function of sliding distance. Wear rate for the first 10 meters of sliding was very high, of the order of $10^{-11} \text{ m}^3/\text{m}$ of sliding. As sliding distance increased, the rate decreased until about 10 000 meters; after this point the rate tended to level off. Even after it leveled off, there was still quite a variation in the wear rate from $4 \times 10^{-14} \text{ m}^3/\text{m}$ to $4 \times 10^{-15} \text{ m}^3/\text{m}$. Sliding speed had no apparent effect on wear rate.

Since the wear rate in the initial stages of sliding was very high, it was postulated that contact stress may have had some effect. Figure 8 plots incremental wear rate as a function of contact stress for each test. Contact stress was determined by using a contact area that was obtained by measuring the area of the transfer film on the rider after the various sliding intervals. Figure 8 shows that wear rate increased with increasing contact stress above a critical value. An empirical fit of the data in figure 8 suggests that this value is approximately $13 \pm 1 \text{ MPa}$.

Rider Transfer

Polymer transfer to the rider was studied by observing the same area with an optical microscope during the intervals when the tests were stopped. Small scratches in the contact area helped locate the same spot. Figure 9 shows the transfer to the same area on the rider from test 5 after 20, 500, and 7500 cycles of sliding. Individual platelets of UHMWPE are seen to be flowing through the contact area and UHMWPE can be seen in the scratches, but it is almost impossible from the optical observations at this point to determine if the rider scar is covered with a thin film of transferred UHMWPE. It can be observed that the scratches are being smoothed (fig. 9(c)), but it cannot be determined whether this was due to a transfer film forming or due to wear of the metallic rider.

After observing the surfaces for longer sliding intervals, it became obvious that considerable transfer was taking place and that the amount increased with sliding duration. The amount and type depended on the sliding speed. At speeds of 1, 10, and 100 rpm very heavy ridges of transfer built up; but at 800 rpm, only thin, flowing transfer films (less than $1 \mu\text{m}$) occurred.

Examples of the different types of transfer are shown in figures 10 to 12. In figure 10, transfer to the rider is shown after 3200 cycles of sliding at 1 rpm against the UHMWPE disk. A considerable buildup of transfer is evident in the rider contact entrance region. Emanating from this material are fibrous crystalline structures. The

origin of these structures is not certain, but they are probably produced on the UHMWPE disk wear track, from which they eventually disengage, and then are collected in the rider entrance. Some are forced into the contact area, where they become attached and give the appearance that they are being produced from rider transfer.

In addition to the fibrous structures, there are ridges of heavy transfer on the rider, and plastically deformed UHMWPE material in the exit region (see blowup in fig. 10). The UHMWPE material appears to have flowed across the rider contact area and coalesced to form the structure shown in figure 10.

The transfer films formed at 10 rpm were very similar to those formed at 1 rpm. The transfer films formed at 100 rpm looked different from those formed at 1 rpm although some fibrous structures were seen. Figure 11(a) shows a typical transfer film for this sliding speed, where heavy ridges of UHMWPE material have built up on the rider.

At 800 rpm the transfer was also different from that at 1 rpm. Figure 11(b) shows typical transfer to the rider that slid at 800 rpm. At this speed, no ridges of UHMWPE occurred. Instead very thin transfer (less than $1 \mu\text{m}$) was observed in which interference fringes could be seen. Figure 12 shows a high-magnification photomicrograph of the transfer to the rider in figure 11(b) that illustrates this type of thin, flowing transfer.

Surface Wear Morphology

For short sliding distances the UHMWPE wear did not appear to depend on sliding speed. Some of the wear features observed on the UHMWPE wear tracks are shown in figure 13. Figure 13(a) shows the raised "roll type" of wear particles, figure 13(b) shows wear grooves and back-transfer particles, and figure 13(c) shows a "glassy looking" wear particle with iridescent speckles in it. Figures 13(c) and (d) also show very thin, plastically flowing surface layers.

The wear surface morphology for the 800-rpm experiments remained the same for long sliding distances; however, for the experiments at 1, 10, and 100 rpm a new wear feature emerged. Figure 14 compares the UHMWPE wear surfaces for the 100-rpm experiments after 65 km (400 kilocycles) of sliding and for the 800-rpm experiments after 245 km (1500 kilocycles) of sliding.

The photomicrograph of the UHMWPE wear track for the 100-rpm-sliding-speed experiment (fig. 14(a)) was taken between crossed polarizing filters. The photomicrograph shows birefringent bands running parallel to the rider sliding direction and birefringent wear debris extending outward from the edge of the wear track. These birefringent bands were not observed at the 800-rpm sliding speed (fig. 14(b)).

It is believed that these bands are caused by the buildup of heavy transfer films (fig. 11(a)). The heavy transfer induced high stresses in localized regions on the UHMWPE disk wear track. Repeated passes over the UHMWPE surface under these high stresses produced orientation and an anisotropic crystalline material. Eventually the crystalline material disengaged from the surface and accumulated at the side of the wear track (fig. 14(a)) or in the rider inlet area (fig. 10). Because grooves were left behind on the wear track, the surfaces were rougher at the lower sliding speeds (figs. 5(a) and (b)).

An additional type of wear particle observed at the 800-rpm sliding speed was a birefringent cylindrical wear particle. This type was found in the exit area of the rider (fig. 15) or outside the disk wear track. The author has also observed this type of wear particle with polyimides (ref. 10). They are postulated to be caused by thin transfer films rolling up as they leave the exit region of the rider or by thin surface layers rolling up and disengaging from the surface.

Another wear phenomenon was observed in one experiment. The UHMWPE disk either had a hard-particle inclusion, or a hard particle was deposited on the wear track during one of the intervals in which the specimens were being examined. Figure 16 shows the wear caused by this hard particle. A deep groove was worn on the metallic rider (fig. 16(a)) by the particle (fig. 16(b)); and subsequently a circumferential ridge occurred on the UHMWPE disk due to the rider groove. The figure points out that third-body wear caused by foreign contaminants can be very detrimental to sliding constituents. This is especially true of soft polymers, which are very susceptible to hard particles embedding in them.

Postulated Friction and Wear Mechanisms

The reason for the higher friction coefficients but lower UHMWPE wear rates at the highest sliding speed (800 rpm) may have been a combination of viscoelastic, molecular relaxation, and temperature effects. At sliding speeds of 1, 10, and 100 rpm, the polymer molecules may have been capable of responding to the strain rate induced by the sliding rider. The molecules tend to inelastically or plastically flow on the surface of the polymer without any undue disruption of the polymer chains themselves. But at 800 rpm the strain rate may have been too great for this type of flow and instead the molecules brittlely fractured. Fracturing of the bonds would result in higher friction than the gradual plastic flow of the molecules. Even though the bonds may have fractured, the UHMWPE wear particles tended to adhere

to the UHMWPE wear surface and helped mitigate wear.

The reason for lower UHMWPE wear at 800 rpm may be associated with the difference in transfer between this speed and the lower speeds. At 800 rpm the thick ridges of transfer present at the lower sliding speeds did not occur. The reason for this may have been the higher temperatures produced or a strain rate too great for the transfer to build up. The absence of the thick transfer ridges eliminated the second wear mechanism (a fatigue-like wear process), and thus the wear rate was less at the highest sliding speed.

Comparison With Other Work

Jones, et al. (ref. 9) have run similar experiments on the identical UHMWPE material (RCH 1000). Their experiments differed in that hemispherically tipped UHMWPE riders were slid against AISI 316L stainless-steel disks with a surface roughness of $0.038 \mu\text{m}$ cla. They found that the friction coefficient initially increased from 0.28 to 0.55 with sliding distance for the first 2 to 3 km of sliding. It then gradually declined during the next 17 km of sliding and eventually stabilized at 0.44 ± 0.07 . The calculated wear rate from their experiments was $(1.6 \pm 0.7) \times 10^{-15} \text{ m}^3/\text{N m}$. In this study, friction coefficient also tended to increase with sliding duration but stabilized at 0.13 ± 0.03 after only 300 meters of sliding. The wear rate was $(2.2 \pm 1.8) \times 10^{-15} \text{ m}^3/\text{N m}$.

Fairly good correlation of wear rates between the two configurations was obtained, but friction coefficients were completely different (0.14 vs 0.44). A possible reason for the difference is that the Jones, et al., experiments used a different stainless steel with a smoother surface finish (316L, $0.038 \mu\text{m}$ cla). Also Jones' experiments were conducted in dry air ($< 50 \text{ ppm H}_2\text{O}$) instead of in moist air ($10\,000 \text{ ppm H}_2\text{O}$). Another possible reason for the difference may have been geometry differences. A similar phenomenon occurred when graphite-fiber-reinforced polyimide (GFRPI) composites were evaluated in these two geometries (ref. 11). The friction coefficient for the GFRPI pin sliding on the metal disk at 25°C was 0.24; the opposite combination gave a friction coefficient of 0.19. As temperature increased, the differences became more pronounced, and at 300°C the friction coefficient for the GFRPI pin sliding against the disk was 0.76, while for the opposite combination it was 0.05.

Atkinson, et al. (ref. 8) have also evaluated the same type of UHMWPE (RCH 1000) in a three-pin-on-disk apparatus. They reported a lower wear rate of $(2.4 \pm 1.8) \times 10^{-16} \text{ m}^3/\text{N m}$, about 10 times less wear. A possible reason for this is that three truncated UHMWPE cones rather than a hemisphere were used, and thus lower initial contact stresses were obtained. Three riders would

also affect transfer film characteristics. An unknown quantity in their tests is the atmosphere: the tests were run in air, but the humidity was not given. In Atkinson's, et al., experiments sliding speed was 0.24 m/s, and applied forces of 25.0 to 155.5 N were evaluated as well as EN 58 J stainless steel counterfaces of 0.015 to 0.120 μm Ra.

Jones, et al. (ref. 9) did not report any microscopic observations of the UHMWPE sliding surfaces; Atkinson, et al. (ref. 8) did. Many of the wear features reported by Atkinson, et al., were also observed in this study—such as “roll type” of wear particles (crescents), back-transfer particles, wear grooves parallel to the sliding direction, and ductile plastic flow.

One type of wear feature not observed by Atkinson, et al., was a “fatigue like” wear particle on the UHMWPE disk that was postulated to be caused by repeated passes over the disk by the ridges of very heavy transfer. This process tended to cause the UHMWPE to crystallize into long, birefringent wear streamers.

Conclusions

Tribological studies at 25° C in a 50-percent-relative-humidity air atmosphere with hemispherically tipped 440C high-temperature stainless-steel riders sliding against ultra-high-molecular-weight polyethylene (UHMWPE) disks led to the following conclusions:

1. Friction coefficient
 - a. Was lowest when contact stresses were highest
 - b. Increased with sliding speed
 - c. Increased as thick transfer films were produced
 - d. Was dependent on specimen contact configuration
2. UHMWPE wear rate
 - a. Was not dependent on sliding speed
 - b. Was dependent on contact stress above stress levels of approximately 13 MPa.
 - c. Was independent of contact stress below stress levels of approximately 13 MPa
3. UHMWPE transfer to rider
 - a. Increased with sliding distance for sliding speeds of 1, 10, and 100 rpm, resulting in the buildup of thick ridges of UHMWPE material.
 - b. Was thin and flowing at 800 rpm and did not build up with sliding distance

4. Wear mechanism

- a. Was adhesion at 800 rpm and for short sliding distances at 1, 10, and 100 rpm
- b. Was fatigue-like for long sliding distances at 1, 10, and 100 rpm, produced by the buildup of UHMWPE transfer ridges on the rider
- c. Was plastic deformation, for high initial contact stresses
- d. Was abrasive when hard particles embedded in the UHMWPE disk and abraded the rider

Lewis Research Center
National Aeronautics and Space Administration
Cleveland, Ohio, April 9, 1981

References

1. Manson, S. S.: New Directions in Materials Research Dictated by Stringent Future Requirements. NASA TM X-67885, 1971.
2. Sliney, H. E.; Jacobson, T. P.; and Munson, H. E.: Dynamic Load Capacities of Graphite-Fiber-Polyimide Composites in Oscillating Plain Bearings to 340° C (650° F). NASA TN D-7880, 1975.
3. Bangs, S.: Foil Bearings Help Air Passengers Keep Their Cool. Power Transmission Design, vol. 15, no. 2, Feb. 1973, pp. 27-31.
4. Blok, H.; and van Rossum, J. J.: The Foil Bearing—A New Departure in Hydrodynamic Lubrication. Lubr. Eng., vol. 9, no. 6, Dec. 1953, pp. 316-320.
5. Ma, J. T. S.: An Investigation of Self-Acting Foil Bearings. J. Basic Eng., vol. 87, no. 4, Dec. 1965, pp. 837-846.
6. Sonstegard, D. A.; Matthews, L. S.; and Kaufer, H.: The Surgical Replacement of the Human Knee Joint. Sci. Am., vol. 238, no. 1, Jan. 1978, pp. 44-51.
7. Dowson, D.; Atkinson, J. R.; and Brown, K.: The Wear of High Molecular Weight Polyethylene with Particular Reference to Its Use in Human Joints. Advances in Polymer Friction and Wear, L. H. Lee, ed., Plenum Press, 1974, pp. 533-551.
8. Atkinson, J. R.; Brown, K. J.; and Dowson, D.: The Wear of High Molecular Weight Polyethylene. Part I: The Wear of Isotropic Polyethylene Against Dry Stainless Steel in Unidirectional Motion. J. Lubr. Technol., vol. 100, no. 2, Apr. 1978, pp. 208-218.
9. Jones, W. R., Jr.; Hady, W. F.; and Crugnola, A.: Effect of Gamma Irradiation on the Friction and Wear of Ultra-High-Molecular-Weight Polyethylene. Wear, vol. 70, no. 1, July 1981, pp. 77-92.
10. Fusaro, R. L.: Comparison of the Tribological Properties at 25° C of Seven Different Polyimide Films Bonded to 440C HT Stainless Steel. NASA TP-1944, 1982.
11. Fusaro, R. L.: Geometrical Aspects of the Tribological Properties of Graphite-Fiber-Reinforced Polyimide Composites. NASA TM-82757, 1982.

TABLE I. - AVERAGE INCREMENTAL FRICTION COEFFICIENTS FOR UHMWPE
DISKS SLIDING AGAINST 440C HIGH-TEMPERATURE STAINLESS-STEEL
HEMISPHERICALLY TIPPED RIDERS

Sliding interval, kilocycles	Test								
	1	2	3	4	5	6	7	8	9
	Sliding speed, rpm								
	1	10	100			800			
Incremental friction coefficient (average)									
0 - 0.02	0.06	0.04	0.08	0.07	0.08	0.08	0.08	0.07	0.09
0.02 - 1.0	.06	.06	.07	.07	.10	.10	.12	.10	.11
1 - 10	.06	.10	.10	.13	.13	.13	.14	.13	.12
10 - 20	----	.11	.13	----	.13	----	.14	----	.13
20 - 60	----	.12	.12	----	.15	----	.13	----	.13
60 - 100	----	.13	.11	----	----	----	----	----	.14
100 - 200	----	----	.11	.15	----	----	----	----	----
200 - 400	----	----	.14	.15	----	----	----	----	----
400 - 600	----	----	.15	.14	.14	----	----	----	----
600 - 1000	----	----	.15	.15	.16	.14	----	----	.13
1000 - 1500	----	----	----	----	.16	----	----	.14	----
1500 - 2000	----	----	----	----	.16	----	----	.15	----
2000 - 3000	----	----	----	----	.17	----	.15	.14	----
3000 - 4000	----	----	----	----	.16	----	----	.14	.12
4000 - 5000	----	----	----	----	----	----	----	----	.11
5000 - 7500	----	----	----	----	----	----	----	----	.11
7500 - 10 000	----	----	----	----	----	----	----	----	.12

TABLE II. - UHMWPE WEAR RATES FOR VARIOUS SLIDING INTERVALS AND SLIDING SPEEDS

Sliding interval, kilocycles	Test								
	1	2	3	4	5	6	7	8	9
	Sliding speed, rpm								
	1	10	100			800			
Incremental wear rate, m^3/m									
0 - 0.02	450×10^{-13}	220×10^{-13}	-----	-----	60×10^{-13}	-----	-----	60×10^{-13}	8×10^{-13}
0 - 1.0	-----	-----	-----	-----	-----	-----	-----	8×10^{-13}	20×10^{-13}
0.02 - 1.0	11	15	-----	-----	11	-----	-----	-----	-----
1 - 10	3	.5	-----	-----	2	-----	2	3	3
10 - 20	-----	.3	0.2×10^{-13}	-----	1	-----	.4	.5	2
10 - 60	-----	-----	-----	-----	-----	0.5×10^{-13}	-----	-----	-----
20 - 60	-----	.2	.1	0.3×10^{-13}	.2	-----	.3	.1	.8
60 - 100	-----	.2	.2	.3	.06	.4	.2	-----	.2
100 - 200	-----	.2	.04	.3	.1	.06	.02	-----	.2
200 - 400	-----	-----	.3	.1	-----	.1	.06	-----	.09
400 - 600	-----	-----	.4	.4	-----	.1	.06	.2	.04
600 - 1000	-----	-----	.3	.05	-----	.1	.03	.06	-----
1000 - 1500	-----	-----	-----	-----	.04	-----	.06	.1	-----
1500 - 2000	-----	-----	-----	-----	.07	-----	.05	.2	-----
2000 - 3000	-----	-----	-----	-----	.08	-----	.06	.2	.06
3000 - 4000	-----	-----	-----	-----	.06	-----	.06	-----	.09
4000 - 5000	-----	-----	-----	-----	-----	-----	-----	-----	.04
5000 - 7500	-----	-----	-----	-----	-----	-----	-----	-----	.04
7500 - 10 000	-----	-----	-----	-----	-----	-----	-----	-----	.04

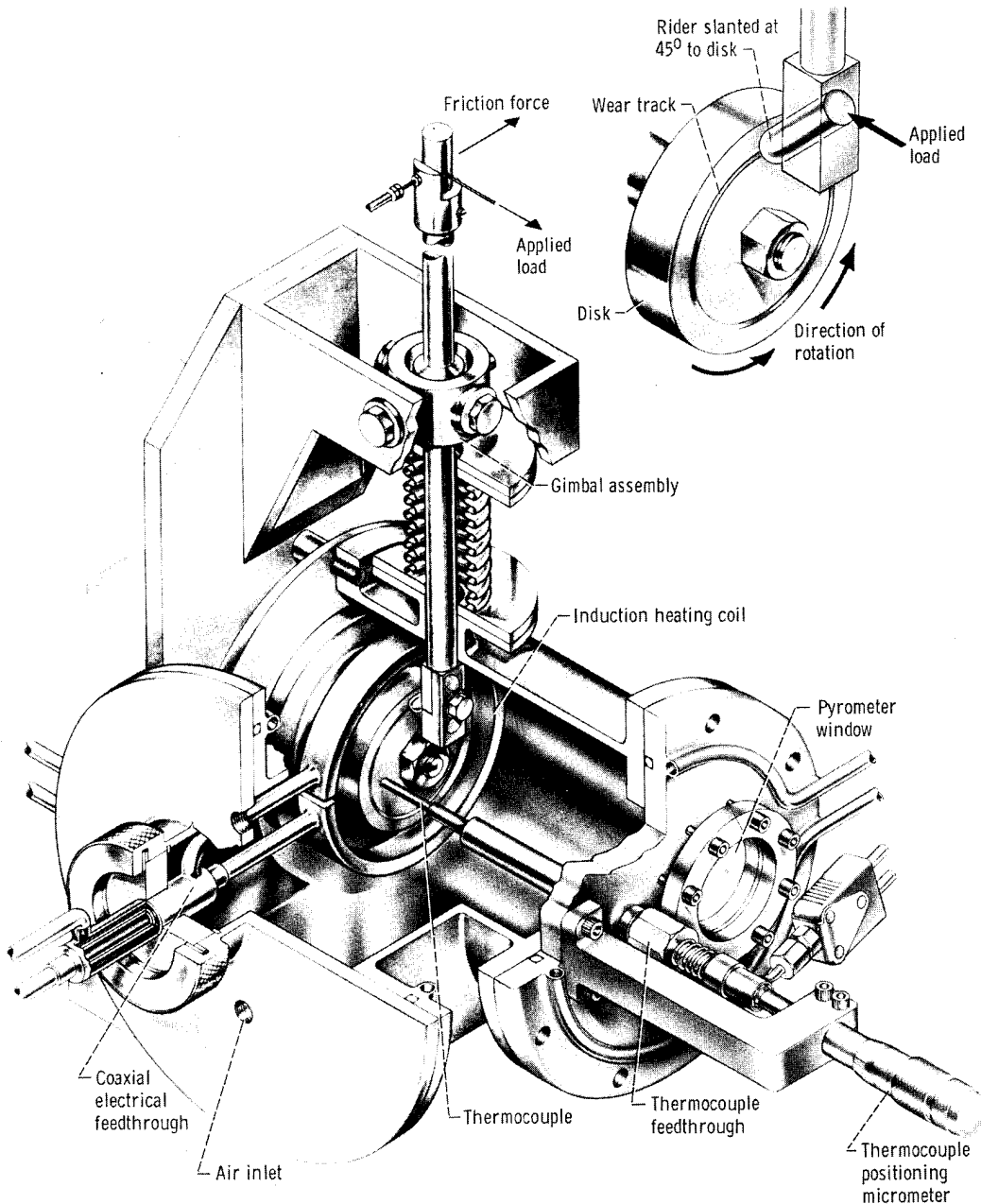


Figure 1. - High-speed friction and wear rig.

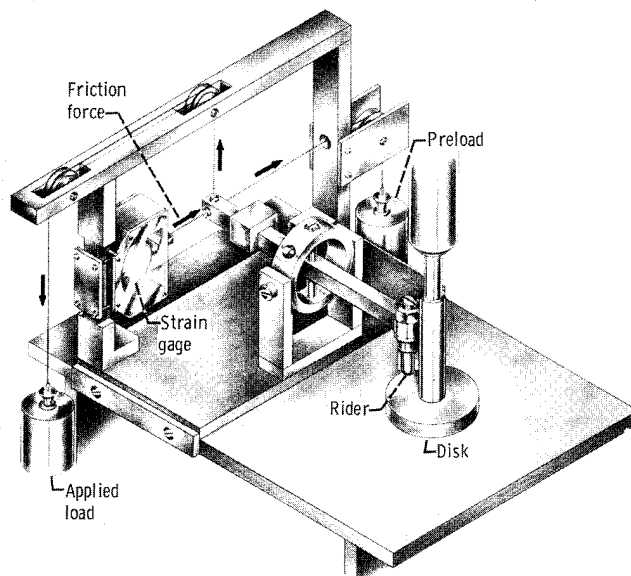


Figure 2. - Slow-speed friction and wear rig.

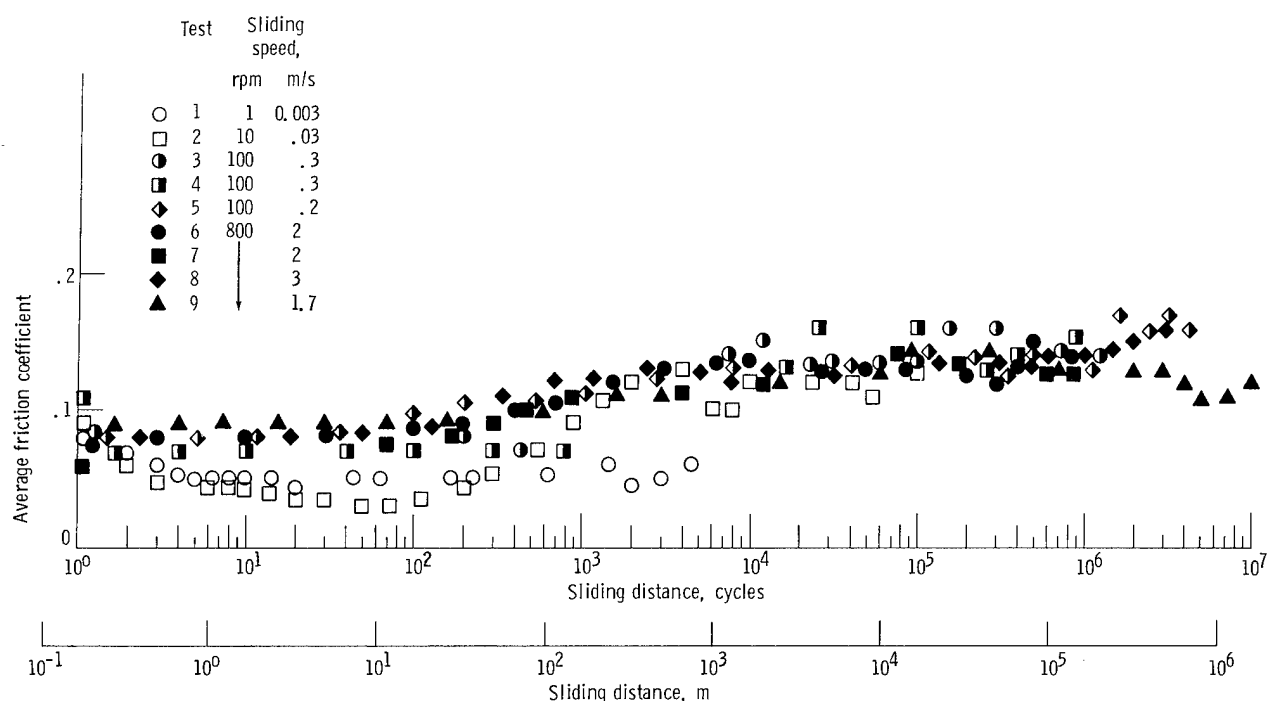


Figure 3. - Average friction coefficient as a function of sliding distance for hemispherically tipped 440C high-temperature stainless-steel rider sliding against UHMWPE disk at various sliding speeds. Temperature, ambient (25°C); load, 9.8 N; atmosphere, 50 percent-relative-humidity air.

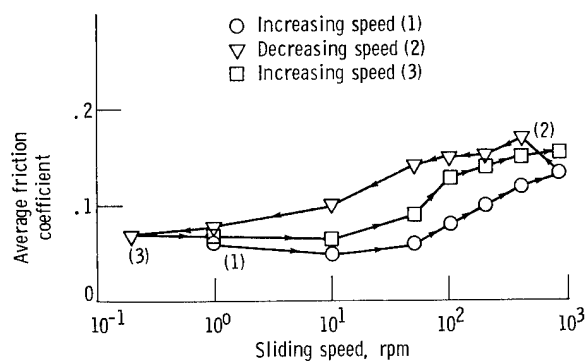


Figure 4. - Average friction coefficient as a function of sliding speed for hemispherically tipped 440C high-temperature stainless-steel rider sliding against UHMWPE disk. Temperature, ambient (25° C); load, 9.8 N; atmosphere, 50-percent-relative-humidity air; sliding time at each speed, 5 min.

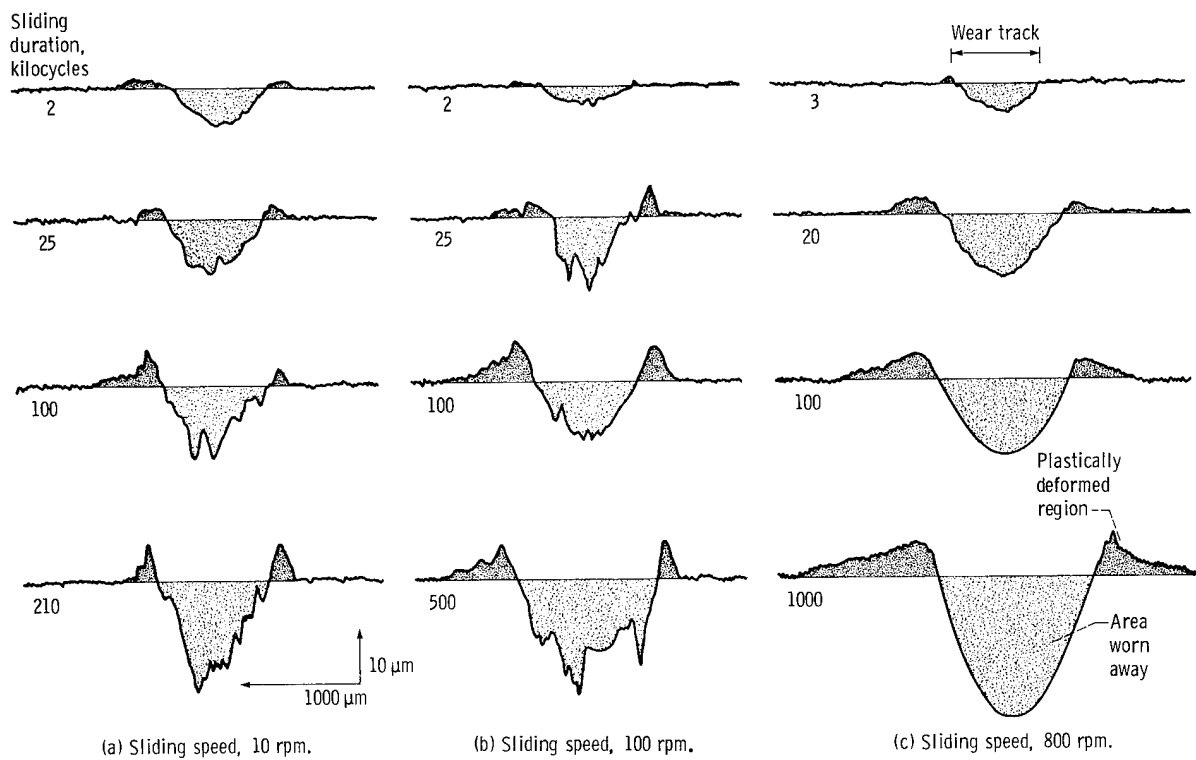


Figure 5. - Surface profiles of wear tracks on U-HMWPE disks after various sliding distances and speeds.

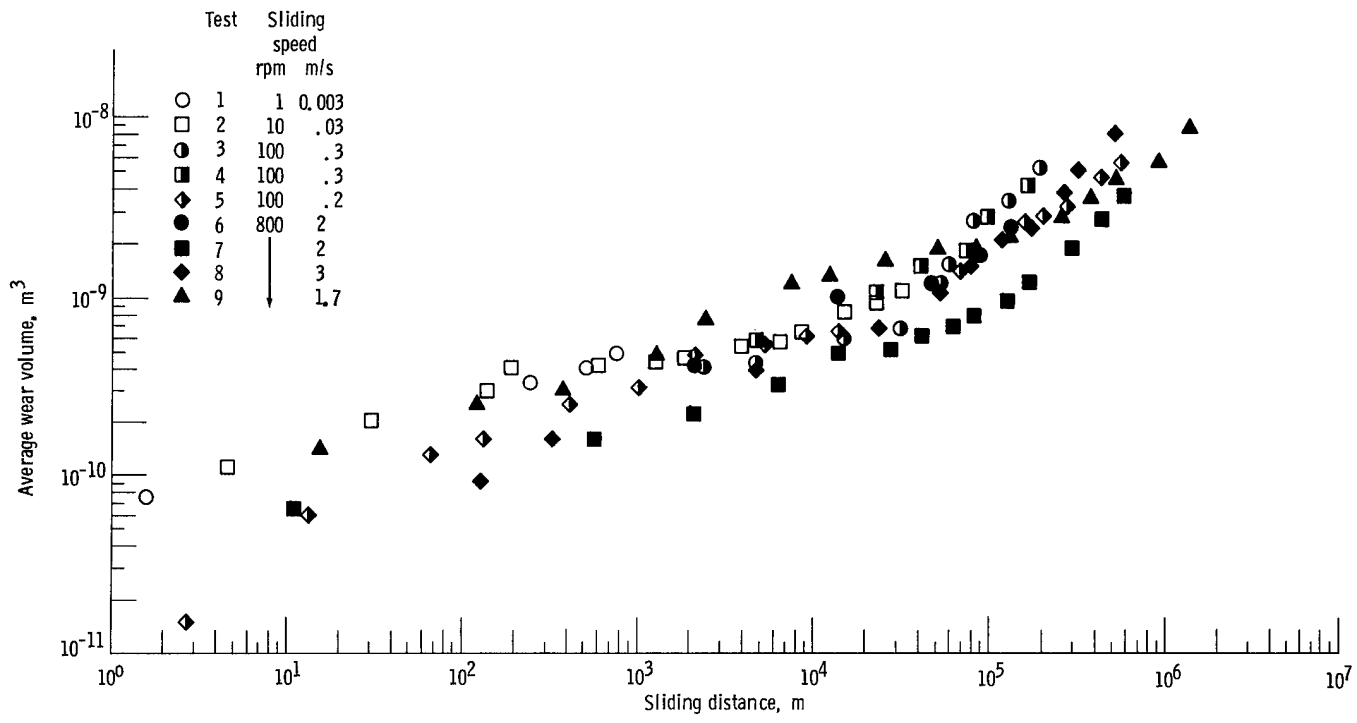


Figure 6. - UHMWPE wear as a function of sliding distance for 9.8-N load applied to hemispherically tipped 440C high-temperature stainless-steel rider for various sliding speeds.

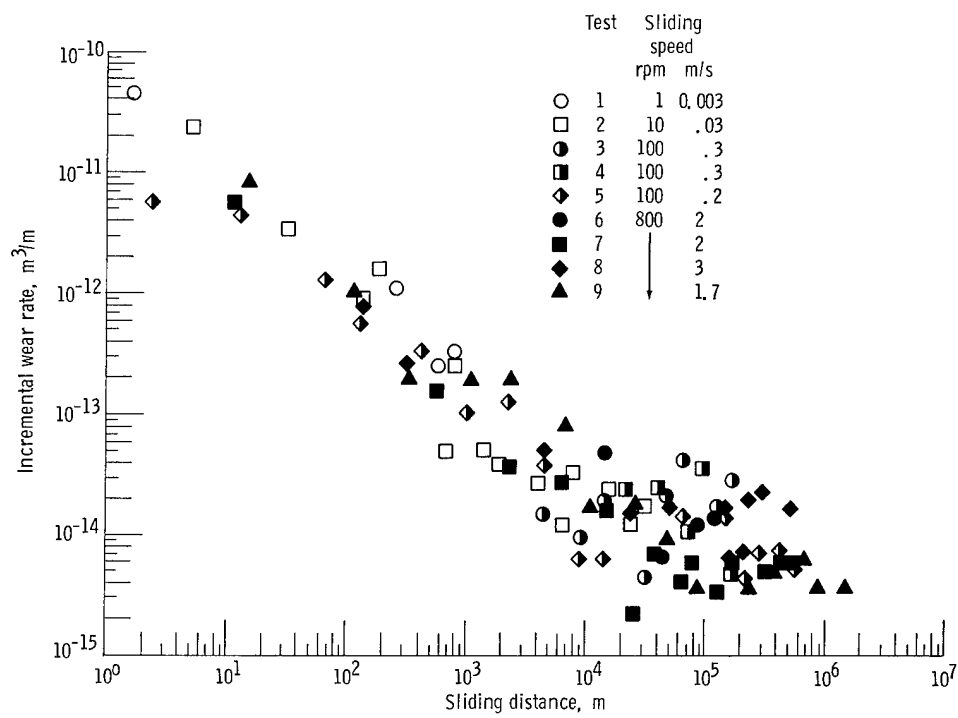


Figure 7. - UHMWPE incremental wear rate as a function of sliding distance for various sliding speeds.

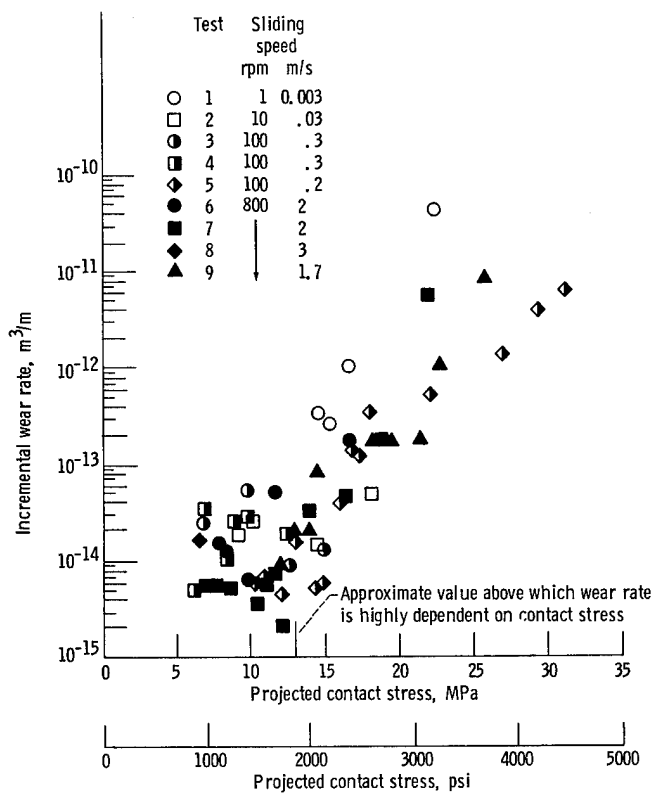
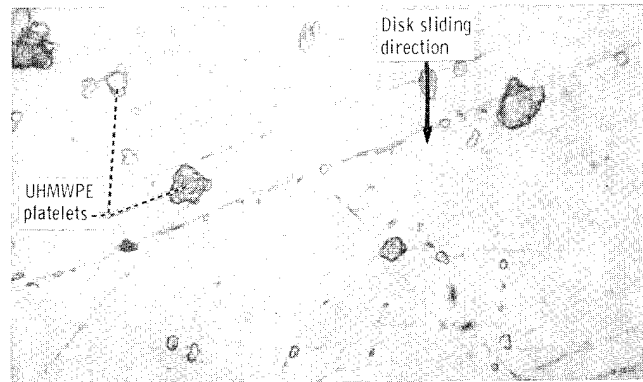
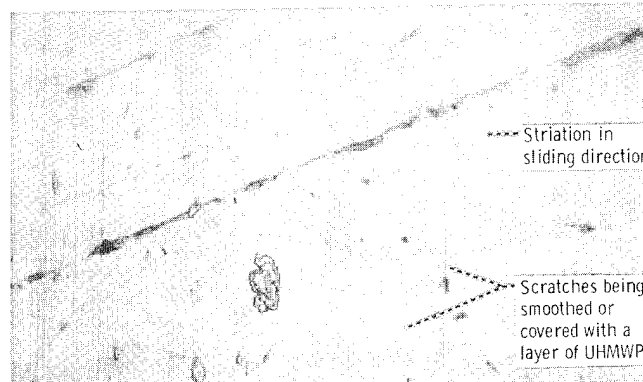


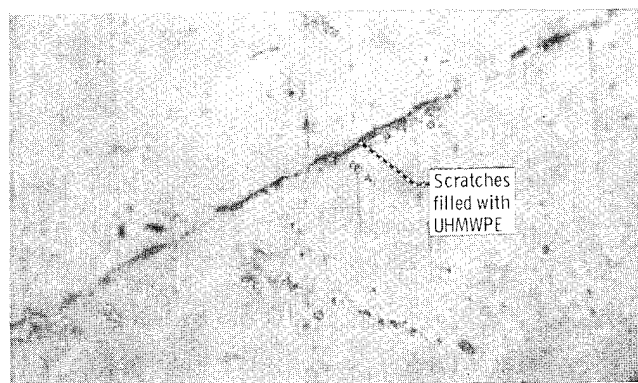
Figure 8. - UHMWPE incremental wear rate as a function of projected contact stress for various sliding speeds.



(a) Sliding duration, 20 cycles (3.3 m).



(b) Sliding duration, 500 cycles (82 m).



(c) Sliding duration, 7500 cycles (1200).

Figure 9. - Transfer to same area on rider from test 5 after various sliding durations on UHMWPE disk. Temperature, ambient (25°C); load, 1 kg; atmosphere 50-percent-relative-humidity air; sliding speed, 100 rpm.

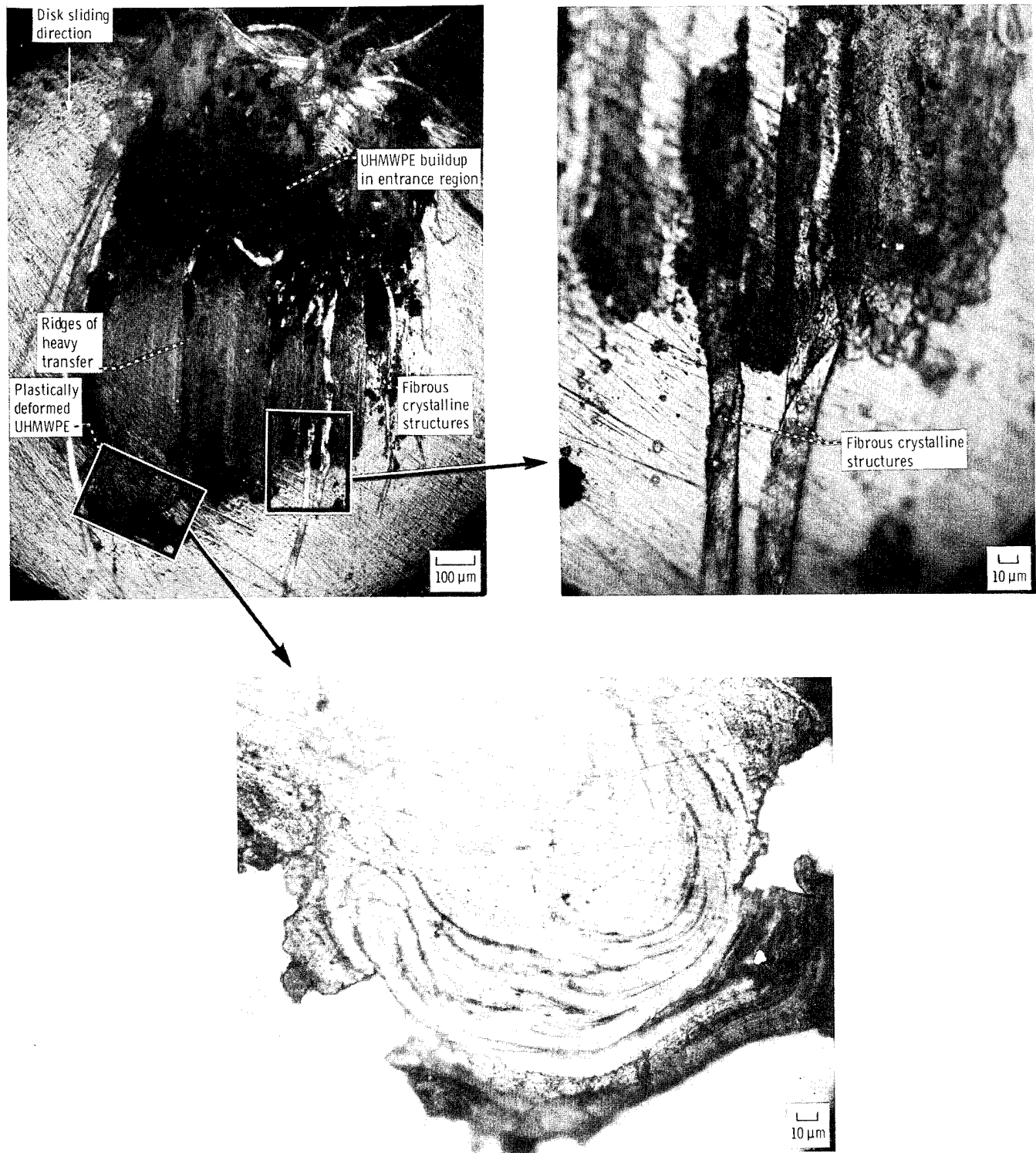
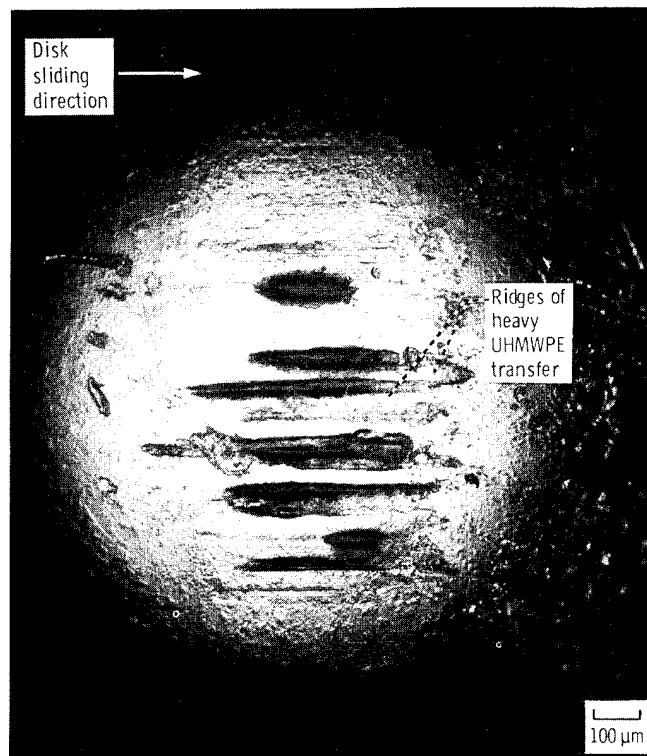
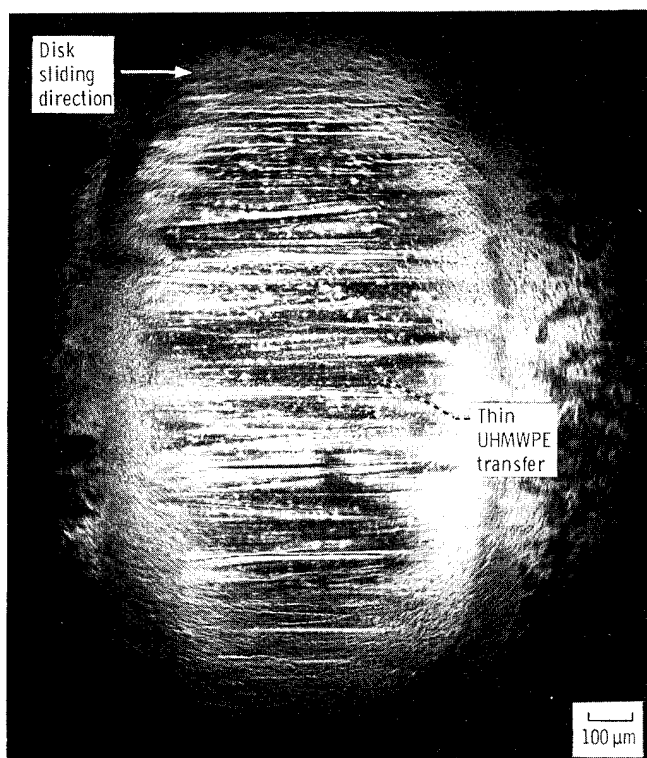


Figure 10. - Film transfer to rider that slid on UHMWPE disk for 3200 cycles (520 m). Sliding speed, 1 rpm.



(a) Sliding duration, 100 kilocycles (16 km); sliding speed, 100 rpm.



(b) Sliding duration, 3000 kilocycles (490 km); sliding speed, 800 rpm.

Figure 11. - Transfer to rider that slid on UHMWPE disk at 100 and 800 rpm.

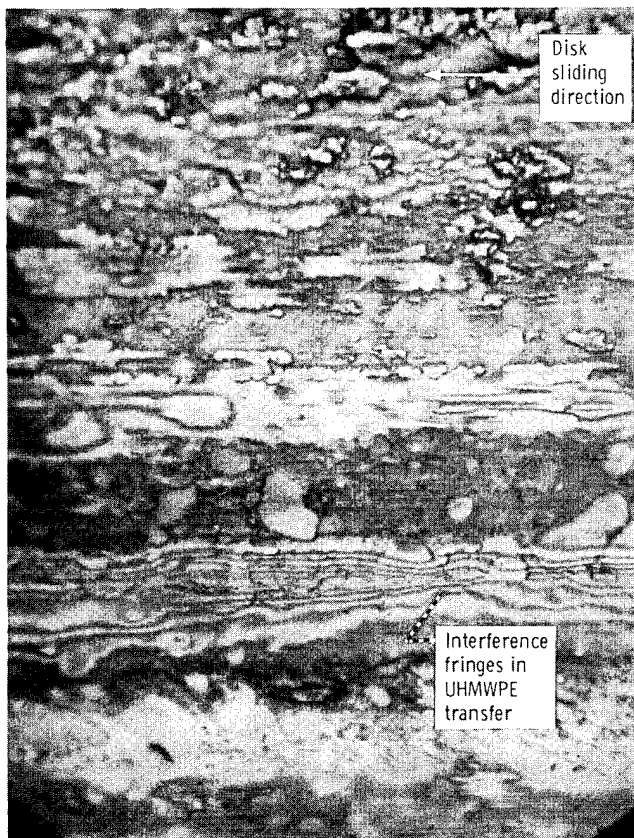
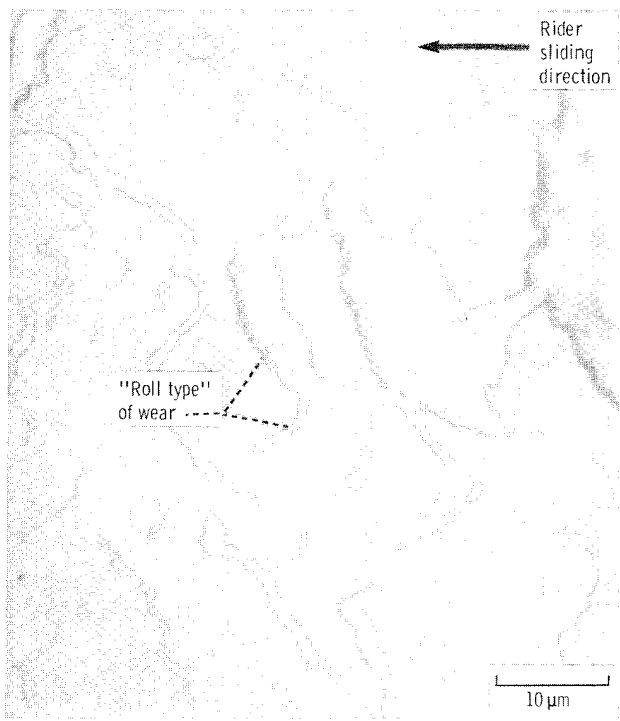
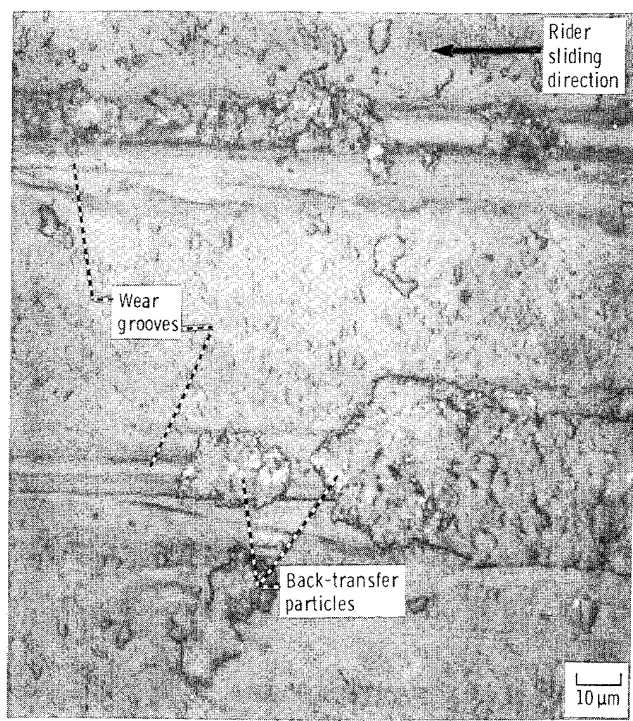


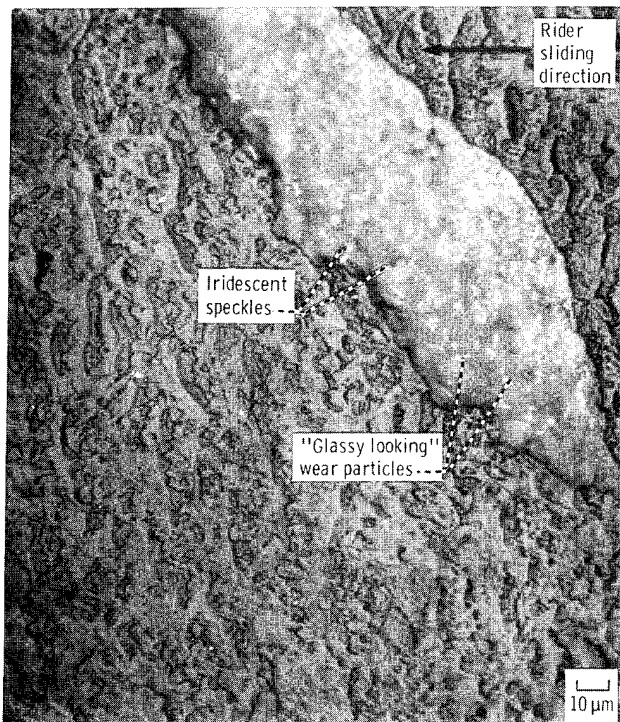
Figure 12. - High-magnification photomicrograph of transfer to rider shown in figure 11(b) after 3000 kilocycles (490 km) sliding. Sliding speed, 800 rpm.



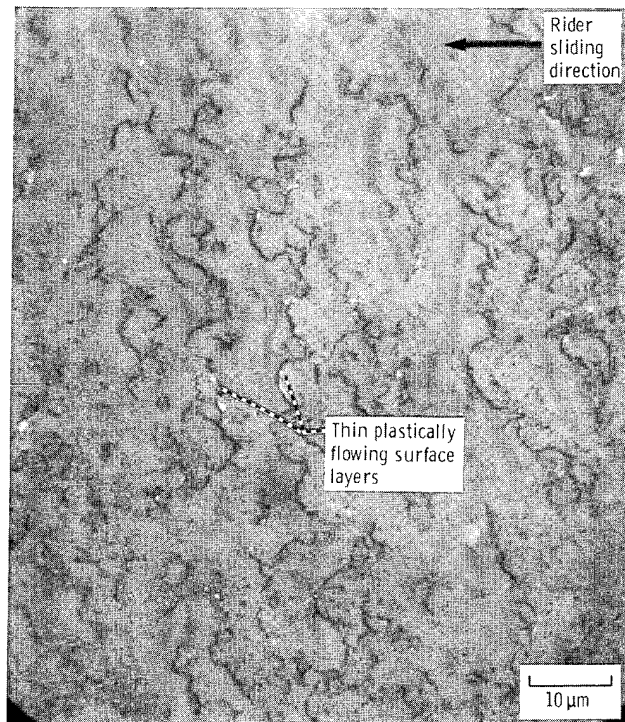
(a) Raised "roll type" of wear particles.



(b) Wear grooves and back transfer.

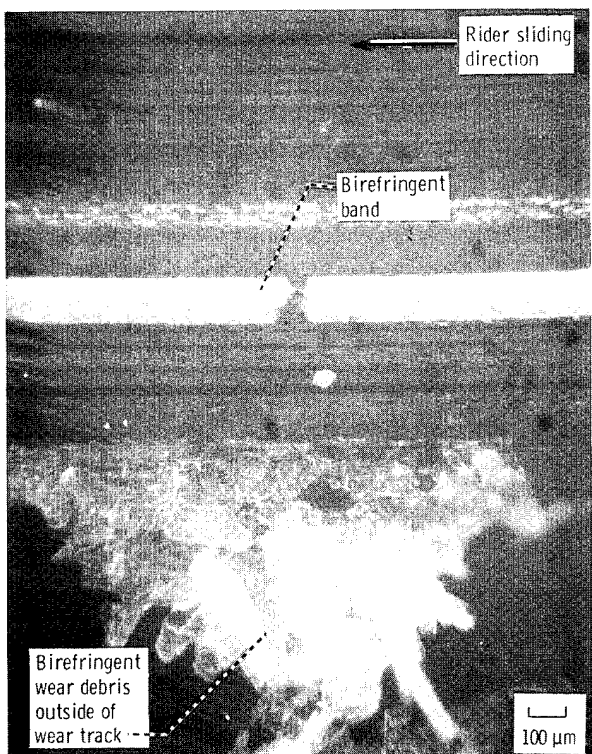


(c) "Glassy looking" wear particles.

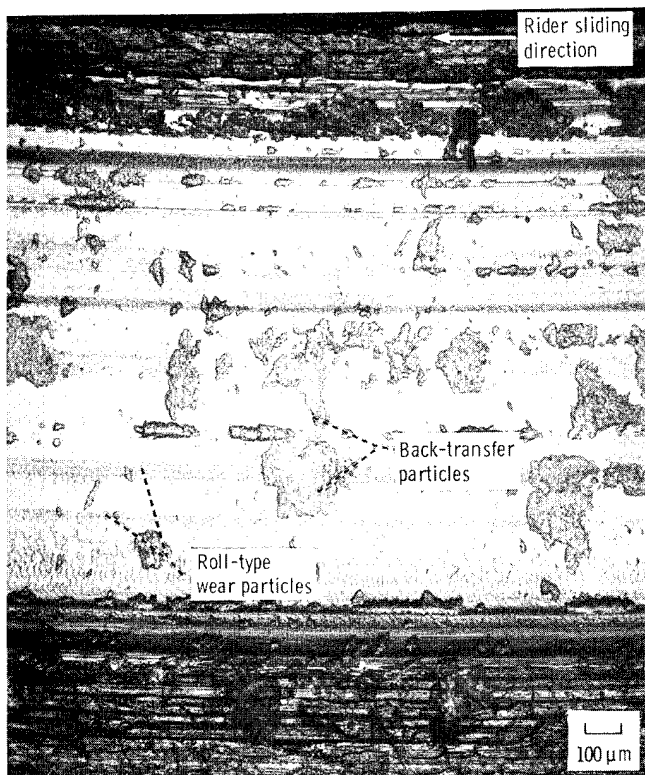


(d) Plastically flowing surface layers.

Figure 13. - Representative photomicrographs showing the various wear features observed on the UHMWPE wear tracks.



(a) Sliding duration, 400 kilocycles (65 km); sliding speed, 100 rpm.
(Photomicrograph taken with specimen between cross Polaroid filters.)



(b) Sliding duration, 1500 kilocycles (245 km); sliding speed, 800 rpm.

Figure 14. - Photomicrographs of wear tracks on UHMWPE disks, showing effect of sliding duration and speed.

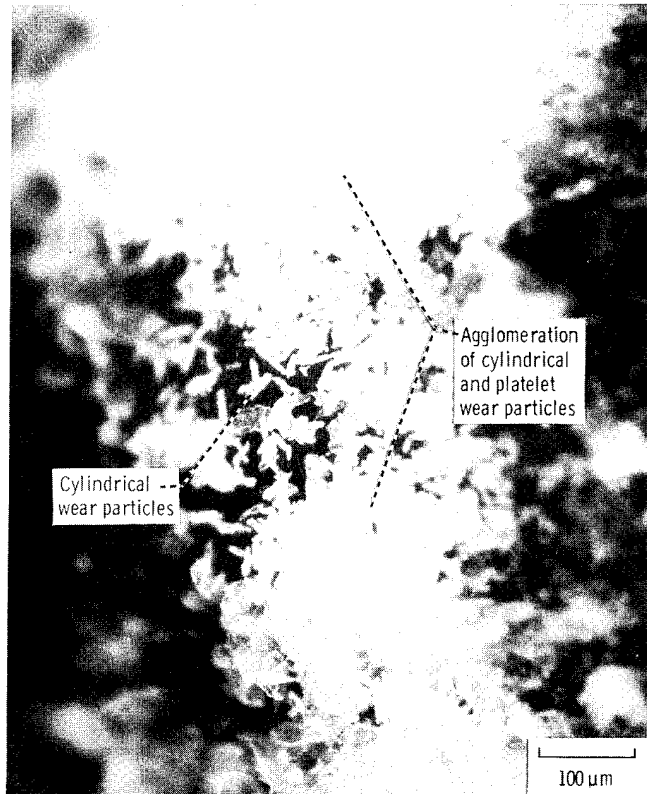
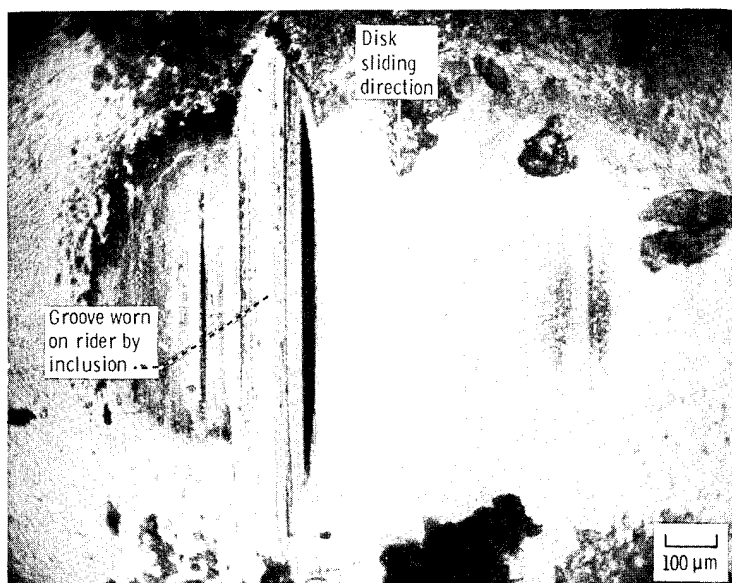
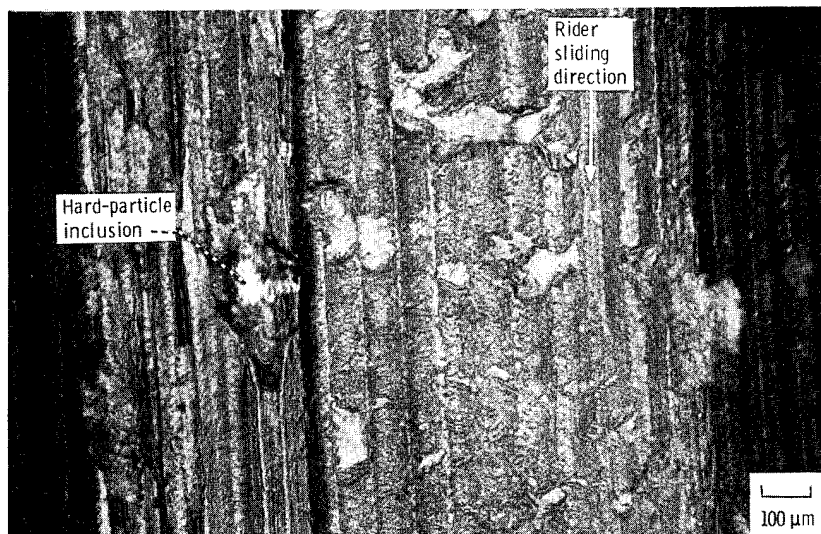


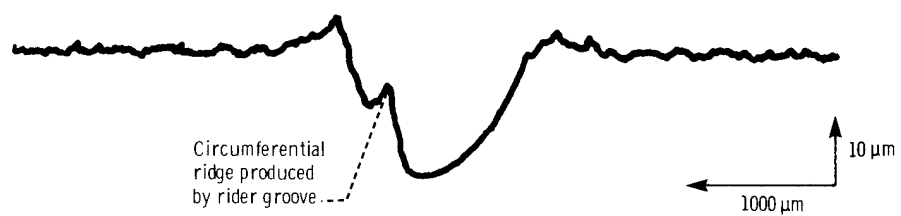
Figure 15. - Birefringent cylindrical wear particles found in exit area of rider that slid on UHMWPE disk at 800 rpm.



(a) Photomicrograph of metallic rider contact area.



(b) Photomicrograph of UHMWPE disk wear track.



(c) Surface profile of UHMWPE disk wear track.

Figure 16. - Photomicrographs and a surface profile of sliding contact areas, illustrating wear caused by embedded hard particle in UHMWPE disk.

1. Report No. NASA TP-2059	2. Government Accession No.	3. Recipient's Catalog No.	
4. Title and Subtitle EFFECT OF SLIDING SPEED AND CONTACT STRESS ON TRIBOLOGICAL PROPERTIES OF ULTRA-HIGH-MOLECULAR-WEIGHT POLYETHYLENE		5. Report Date November 1982	
7. Author(s) Robert L. Fusaro		6. Performing Organization Code 505-32-42	
9. Performing Organization Name and Address National Aeronautics and Space Administration Lewis Research Center Cleveland, Ohio 44135		8. Performing Organization Report No. E-1060	
12. Sponsoring Agency Name and Address National Aeronautics and Space Administration Washington, D.C. 20546		10. Work Unit No.	
		11. Contract or Grant No.	
		13. Type of Report and Period Covered Technical Paper	
		14. Sponsoring Agency Code	
15. Supplementary Notes			
16. Abstract A pin-on-disk apparatus was used to investigate the effect of sliding speed on the friction, wear, and transfer film characteristics of hemispherically tipped AISI 440C high-temperature (HT) stainless-steel riders sliding against ultra-high-molecular-weight polyethylene (UHMWPE) disks. The surface morphology of the wear track was studied to determine possible wear mechanisms. Geometry effects were determined by comparing the results to those of others who used different specimen configurations. The results indicate that sliding speed, sliding distance, contact stress, and specimen geometry can all markedly influence the tribological properties of UHMWPE.			
17. Key Words (Suggested by Author(s)) Dry friction; Wear; Lubrication; Polyethylenes; Wear tests; Coefficient of friction; Self lubrication; Self-lubricating materials; Surface properties		18. Distribution Statement Unclassified - unlimited STAR Category 27	
19. Security Classif. (of this report) Unclassified	20. Security Classif. (of this page) Unclassified	21. No. of Pages 21	22. Price* A02

* For sale by the National Technical Information Service, Springfield, Virginia 22161

NASA-Langley, 1982